RAPID COMMUNICATIONS

PHYSICAL REVIEW E VOLUME 53, NUMBER 2 FEBRUARY 1996

# Hopf bifurcation by frustrated drifts

Walter Zimmermann and Rainer Schmitz
*Institut für Festkörperforschung, Forschungszentrum Jülich, D-52425 Jülich, Germany*
(Received 10 May 1994)

We describe, with a Hopf bifurcation induced by frustrated drifts, a phenomenon in pattern formation. This generic effect occurs in systems with broken continuous translational and reflection symmetry. Above the bifurcation point periodic or aperiodic motion occurs depending on the actual manifestation of the symmetry breaking. The qualitative aspects of the phenomenon are discussed within a generalized Swift-Hohenberg equation. In addition, based on detailed calculations, also a geometry for a Rayleigh-Bénard experiment is proposed, where the effect can be investigated experimentally.

PACS number(s): 47.20.−k, 03.40.Gc, 05.45.+b

## I. INTRODUCTION

The understanding of complex phases as well as complex spatiotemporal behavior of matter is one of the central issues in physics [1,2]. The elaboration of the variety of phases of matter is mainly a topic of physics at thermal equilibrium [2]. When driven far from thermal equilibrium, the various inner degrees of freedom of complex fluids, such as in binary fluid mixtures or in liquid crystals, lead to rich bifurcation scenarios [1]. Especially the various bifurcations from a simple basic state allow the application of perturbational methods and contribute to the popularity of complex fluids for investigations of spatiotemporal complexity. Instead of complex fluids, one might use simple fluids with inhomogeneous container boundaries, enforcing a lower symmetry. We predict a geometry with broken symmetries, where the first bifurcation changes from a stationary into an oscillatory one. The nonlinear solutions behavior can be temporal periodic or aperiodic in space-time. These phenomena are described perturbatively in terms of amplitude equations. It is an example of geometrically induced spatiotemporal complex behavior occurring already at the first bifurcation, which also shares common features with coupled oscillator systems [3] and a variant of the Kuramoto-Sivashinsky equation [4].

Broken spatial symmetry occurs in Rayleigh-Bénard convection (RBC), for example, when the top and the bottom plate have some characteristic undulation (Fig. 1). If the top and bottom boundaries have undulations of the same wave number and if they are also in phase [Fig. 1(a)], then stationary convection sets in above a critical temperature difference, $\Delta T = T_u - T_b > \Delta T_c$, between the temperature at the top ($T_u$) and the bottom ($T_b$) plate. A phase difference between the top and the bottom plate, as indicated in Figs. 1(b) and 1(c), leads to drifting convection rolls to the left or to the right depending on the sign of the phase shift [5].

In experiments, symmetries for convection are often weakly broken by irregularities at container boundaries or by the porosity in a saturated porous medium. The irregularities are expected to be of a statistical nature. Nevertheless, some aspects of those irregularities may be modeled by periodic undulations in the container boundaries. Boundary undulations, inducing homogeneous drifts as indicated in Figs. 1(b) and 1(c), are less appropriate for modeling aspects of irregularities, such as, for instance, a vanishing spatial mean value for drifts induced by irregularities. Therefore, we consider here a situation corresponding to a geometry where the phase shift $\varphi$ between the wavy top and bottom boundary varies periodically in space, however, slow on the scale of the convection rolls. We show that a phenomenon, which we call the *Hopf bifurcation by frustrated drifts*, is a consequence. It is essential for the occurrence of such time-dependent solutions that the space-dependent phase shift acts on a spatially periodic pattern near onset.

## II. MODEL EQUATION

At first (for applications to Rayleigh-Bénard convection see below) we illustrate the qualitative aspects of the interplay of spatially periodic drifts and spatially periodic patterns near onset within the following models in one dimension:

$$\partial_t u = [\varepsilon + \mathscr{L}_0 + M(x)\partial_x]u - u^3. \tag{1}$$

$M(x)\partial_x$ is a $2\pi$-periodic "drift" and breaks the spatial translational symmetry. With the linear operator $\mathscr{L}_0 = \partial_x^2$ Eq. (1)

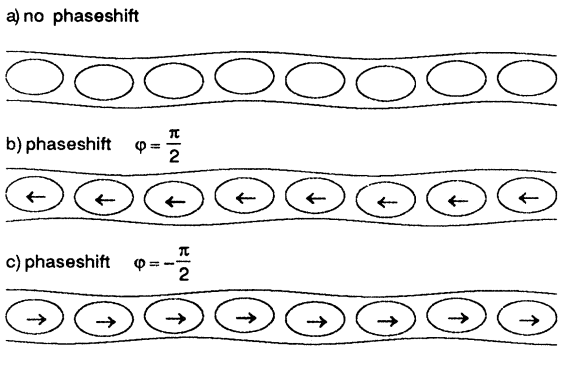


FIG. 1. A sketch of a Rayleigh-Bénard convection cell with wavy top and bottom boundaries. Periodic in phase undulation of the boundaries leads to a stationary onset to convection rolls (a). As indicated in (b) and (c), a phase difference between the two boundary undulations leads above threshold to drifting convection rolls and the drift direction depends on the sign of the relative phase $\varphi$.

 

corresponds to a real Ginzburg-Landau equation (GL) and with $\mathscr{L}_0=-(q_0^2+\partial_x^2)^2$ Eq. (1) corresponds to a generalized Swift-Hohenberg equation (SH) [1]. If not stated otherwise we choose $M(x)=2G\cos(2kx+\varphi)$.

For a constant drift $M\partial_x u[M(x)=\text{const.}]$, the drift term can be removed in both cases by transforming into the comoving coordinate frame. For a single periodic $M(x)$ with vanishing spatial mean $\langle M(x)\rangle=0$ the drifts are frustrated. This frustration leads to a time-dependent solutions behavior above some critical amplitude of $M(x)$ in the case of the generalized SH equation. For the Ginzburg-Landau case, however, where the spatially periodic drifts act on a homogeneous phase transition, not on a spatially periodic one, no time dependence is induced. If $M(x)$ is not single periodic the solutions behavior of the generalized SH equation near the onset is more complex, as described below.

For periodic $M(x)$ the solutions of the linear part of Eq. (1) are either symmetric $u_s(x)=u_s(x+\lambda)$ with respect to a translation by $\lambda=\pi/k$ or antisymmetric $u_a(x)=-u_a(x+\lambda)$. [$u_s(x)$ correspond to the harmonic and $u_a(x)$ correspond to the subharmonic solutions.]

### A. Linear stability

In the homogeneous limit $G=0$, the linear part of Eq. (1) is solved by $u=F\exp[\sigma t+iqx]$. This leads in the neutrally stable case $\sigma=0$ to an expression for the neutral curve of the Ginzburg-Landau equation, $\varepsilon_0^{GL}=q^2$, and for the Swift-Hohenberg equation, $\varepsilon_0^{SH}=(q_0^2-q^2)^2$. These neutral curves have minima at the critical values $q_c^{GL}=0$, $q_c^{SH}=q_0$, and $\varepsilon_c=0$.

In the presence of a spatially periodic drift term the linear solutions can be written in terms of a Floquet-Bloch expansion $u(x,t)=e^{\sigma t+iqx}\sum_{l=-N}^{N}F_l\exp(ilkx)+\text{c.c.}$ (with $-k<q-q_0<k$ and c.c.=complex conjugate). Harmonic and subharmonic parts with respect to the external modulation separate in the linear part of Eq. (1) and give rise to two different thresholds.

The main difference between the GL and SH version of Eq. (1) can be calculated within a subharmonic two mode ansatz $u=\exp[\sigma t+iqx](F_1\exp[ikx]+F_{-1}\exp[-ikx])+\text{c.c.}$ This leads to the following dispersion relations for $q=q_0$:

$$\sigma_{1,2}^{GL}=\varepsilon-k^2\pm G, \tag{2}$$

$$\sigma_{1,2}^{SH}=[\varepsilon-4k^2-k^4]\pm[16k^6-G^2(q_0^2-k^2)]^{1/2}. \tag{3}$$

For the GL equation the eigenvalue $\sigma$ in Eq. (2) is always real, whereas for the SH equation the eigenvalue becomes complex for $G>4k^3/\sqrt{q_0^2-k^2}$. This reflects the essential property that spatially periodic drifts lead only to time-dependent solutions when they interact with a spatially periodic solution. In Fig. 2 the thresholds $\varepsilon_c\equiv\varepsilon(\text{Re}[\sigma]=0)$, calculated with many modes of the Fourier expansion, are shown for the symmetric (solid and dashed line) and the antisymmetric solutions (dash-dotted line) as a function of the modulation strength and for a fixed modulation wave number $k=1/16$. At the modulation strength where both thresholds cross each other, both linear instabilities compete with each other and one has a codimension-2 bifurcation [1].

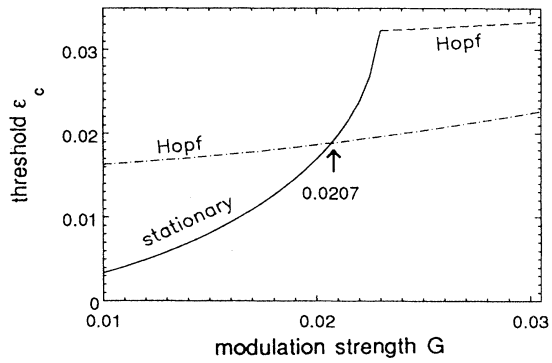


FIG. 2. The thresholds of the harmonic (solid lines) and the subharmonic solutions (dash-dotted) of Eq. (1) are given as function of the modulation strength $G$ and at the fixed modulation wave number $k=1/16$. The bifurcation of the harmonic solutions from $u\equiv 0$ is stationary at smaller values of the modulation strength $G$ (solid line) and oscillatory for larger $G$ values (dashed line). The subharmonic solution (dash-dotted) shows a Hopf bifurcation in the whole plotted $G$ range. The cross point between the two thresholds is a codimension-2 bifurcation [1] being approximately located at $G_{CTP}\simeq 0.020\,72$.

### B. Eigenmodes

At the Hopf bifurcation the linear solution of Eq. (1), $u=e^{iq_cx}\Sigma_l[Ae^{i\omega_c t}F_l^{+}+B^{*}e^{-i\omega_c t}F_l^{-}]e^{ilkx}+\text{c.c.}$, is a superposition of left (LTW's) and right traveling waves (RTW's) as shown in Fig. 3. The envelope of these traveling waves is spatially fixed with respect to the external modulation, whereas the phase is moving. The envelope of the LTW reaches its maximum in the range where the RTW has its minimum. This relative phase shift of the spatial modulation reduces the nonlinear interaction between both modes and coexistence becomes possible, namely, standing waves. This is different from other systems, such as for example in binary fluid convection and electroconvection, where only one extended unmodulated traveling mode survives.

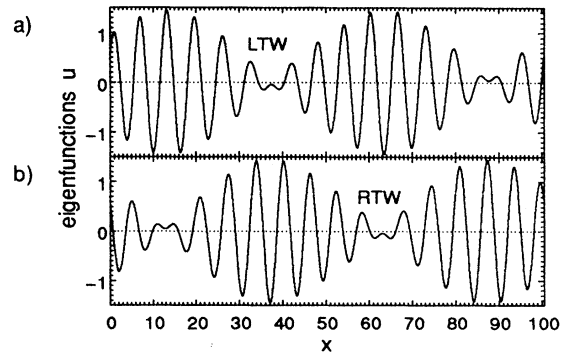


FIG. 3. The eigenfunctions of the linear part of Eq. (1) in the range $0<x<2\pi/k$ at a Hopf bifurcation. Part (a) shows the left and part (b) the right traveling wave just above the codimension-2 point $G_{CTP}$ at the parameters $G=0.022$ and $k=1/16$. Both eigenfunctions are subharmonic with respect to the external modulation $M(x)=2G\cos(2kx)$.

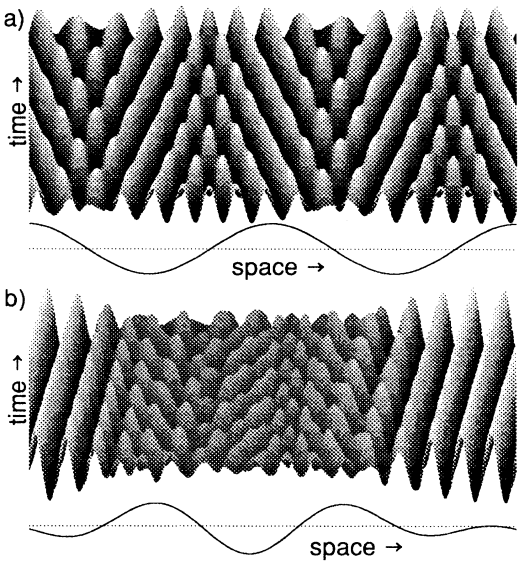


FIG. 4. The solution $u(x,t)$ of Eq. (1) is shown just above a Hopf bifurcation in a space-time plot. As shown in part (a) $u(x,t)$ is periodic in time for a single periodic modulation $M(x)$ and aperiodic for a two periodic modulation $M(x)$ as shown in part (b).

### C. Nonlinear solution

Above a Hopf bifurcation by frustrated drifts a typical temporal behavior of a nonlinear standing wave is shown in Fig. 4(a). Equation (1) was solved for a single periodic modulation $M(x)=2G\cos(2kx)$ with the parameters $\varepsilon=0.05$, $G=0.05$, and $k=1/16$. Just above threshold this solution corresponds roughly to a superposition of the two eigenmodes given in Fig. 3 and the temporal behavior at any space point $x$ is nearly harmonic. Increasing the value of $\varepsilon$ the temporal behavior of the solution at each space point becomes more and more anharmonic. This happens especially near the secondary bifurcation, leading to the stationary solution. In $x$ regions, where both traveling wave eigenmodes shown in Fig. 3 have comparable amplitudes, the nonlinear solution resembles an extended standing wave, otherwise it has the shape of modulated traveling waves [see Fig. 4(a)]. The regions in Fig. 4(a) with standing wave behavior have a similar form as defects between the LTW's and RTW's, namely, sinks and sources. These similarities, however, should not be overemphasized, because the eigenmodes in Fig. 3 are already of that spatially modulated form. The transition from standing waves to the stationary solution at large $\varepsilon$ values is of first order with a large hysteresis.

A two periodic drift coefficient $M(x)=2G\cos(2kx+\pi/2)+2G_2\cos(3kx+\pi/4)$ leads, instead of standing waves, to aperiodic and chaotic motion as indicated in Fig. 4(b) (for $G=0.045$, $G_2=0.046$, $k=1/16$, and $\varepsilon=0.068$).

With the ansatz $u=A\exp(iq_0x)+\text{c.c.}$, $M(x)\approx O(\varepsilon)$, $k\approx O(\varepsilon^{1/2})$, and $q_0=1$ from Eq. (1) the following generalized Ginzburg-Landau equation can be derived:

$$\partial_t A=[\varepsilon+iM(x)+4\partial_x^2]A-3|A|^2A, \tag{4}$$

which has the same solution behavior as the starting equation, apart from small quantitative differences ($i$ is the imaginary unit). Similar generalized GL equations are expected for systems with comparable broken symmetries. An example is discussed below for Rayleigh-Bénard convection. The described properties are generic and not specific to the SH equation. Essential for the occurrence of the Hopf bifurcation by frustrated drifts is the interplay between the periodic instability and the spatially periodic drift, whereas the wavelength of the periodic drift is much larger than that of the instability ($k\ll q_0$).

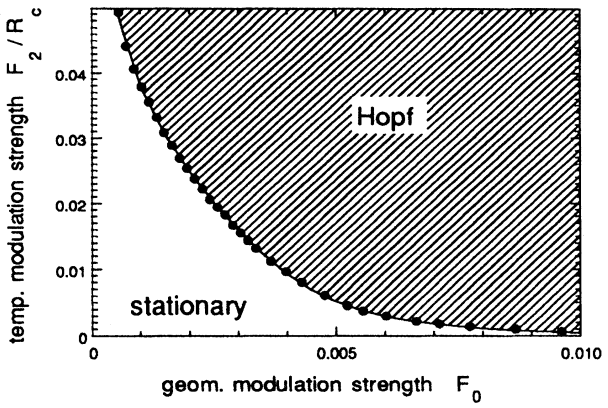


FIG. 5. Rayleigh-Bénard convection: Bifurcation diagram for a top wavy boundary and a spatially modulated temperature at the bottom boundary. In the shaded range the onset of convection is oscillatory (Hopf bifurcation by frustrated drifts), and otherwise stationary. The bottom temperature is modulated with an amplitude $F_2$ (see text) and with a wave number $k_2=3k$. The top boundary is undulated with an amplitude $F_0$ and with a wave number $k_0=2k$ ($kd=0.1$ and $d$=thickness). The dots are directly calculated from the Navier-Stokes equations (see [6]) and the solid line from the linear part of the generalized amplitude equation ( 5).

The similarities of Eq. (4) with model equations for coupled oscillator families [1,3], especially for a random function $M(x)$, are obvious and will be discussed elsewhere.

## III. RAYLEIGH-BÉNARD CONVECTION

For a Rayleigh-Bénard cell with two wavy boundaries and a phase shift between both, as shown in Fig. 1, drifting convection rolls have been observed [5]. We find that a drifting pattern in RBC can also be induced by a combination of an undulated boundary and a modulated temperature at the other boundary. For instance, by combining an undulated top boundary located at $z=d(1+H_0)$ [with $H_0=F_0\cos(k_0x)$] and a modulated temperature at the bottom boundary at $z=0$, $T_b=\bar{T}_b+H_2(x)(\bar{T}_b-T_u)/R_c^f$ [with the dimensionless $H_2(x)=F_2\cos(k_2x+\varphi_2)$, and $R_c^f=27\pi^4/4$ being the critical Rayleigh-number for free-slip boundary conditions], with equal modulation wave numbers $k_0=k_2$ as well as finite phase shift $\varphi_2\neq 0$ [6].

A combination of the undulation of the top boundary $H_0(x)$ with wave number $k_0=2k$ and a modulation of the temperature at the bottom boundary $H_2(x)$ with $\varphi_2=\pi/2$ and $k_2=3k$ leads to spatially periodic virtual drift directions, just as for our model in Eq. (1) or in Eq. (4).

Near the onset of convection, an equation for the envelope

of the RBC rolls can be derived by a perturbation calculation [7]. For the expansion one uses the small parameter $\varepsilon=(\Delta T-\Delta T_c)/\Delta T_c$, which measures the distance from the critical temperature difference at which the convection sets in. Assuming additionally small modulation amplitudes and modulation wave numbers $H_i(x),(k/q_c)\propto\varepsilon^{1/2}$ ($q_c$ is the wave number of the convection rolls) the perturbation calculation provides the following amplitude equation for stress free boundary conditions:

$$\tau_0\partial_t A_0=\left[\varepsilon-\frac{35}{6}H_0^2+3H_0+\left(1+\frac{5}{3}H_0\right)\frac{H_2}{R_c}+i\frac{\sqrt{2}}{\pi}\left(\frac{271}{576}\partial_x H_0-\frac{5}{192R_c}\partial_x H_2\right)\right]A_0+\left[i\frac{2\sqrt{2}}{3\pi}\left(H_0-\frac{1}{R_c}H_2\right)\partial_x+\xi_0^2\partial_x^2-\alpha|A_0|^2\right]A_0 \tag{5}$$

with $\xi_0^2=\alpha=8/3\pi^2$ and $\tau_0=9\pi^2/2R_c$.

An analysis of the linear part of Eq. (5) as well as a full analysis of the Navier-Stokes equations [6] shows that by increasing the modulation amplitudes in RBC the onset of a stationary periodic pattern can be changed via frustrated drifts into an oscillatory one. Figure 5 displays the parameter range for RBC with stress free boundary conditions where the onset of convection is oscillatory (shaded region) and otherwise stationary. The modulation wave numbers were fixed at $k_2=3k$, $k_0=2k$, and $kd=0.1$ (with $d$ the distance between top and bottom boundary). The solid line in Fig. 5 is calculated from the linear part of Eq. (5), whereas the dots are calculated from the equations of motion for thermal convection. There is also no qualitative difference between the stress free and realistic nonslip boundary conditions for the velocity field at the boundaries [6].

## IV. DISCUSSION AND CONCLUSION

We described an example, where geometrically induced broken symmetries lead to a rich bifurcation behavior via the Hopf bifurcation by frustrated drifts. The essential features, described in terms of a generalized Swift-Hohenberg model, are generic for systems having a spatial periodic first instability and similar broken symmetries. Based on detailed calculations, we also predict this effect for an appropriately designed Rayleigh-Bénard convection experiment. Further candidates are the Taylor-Couette system or thermal convection and electroconvection in nematic liquid crystals having a spatially periodic pretilt angle of the director with respect to the top and bottom boundary. For convection in nematic liquid crystals with less well defined surface alignment, Hopf bifurcation by frustrated drifts may lead to new experimental scenarios.

## ACKNOWLEDGMENTS

We thank H. Müller-Krumbhaar for useful discussions and M. Zimmer for careful reading of the manuscript. This work was supported by the DFG.

[1] P. Manneville, *Dissipative Structures and Weak Turbulence* (Academic, London, 1990); M.C. Cross and P.C. Hohenberg, Rev. Mod. Phys. **65**, 851, (1993).

[2] P. G. de Gennes and J. Prost, *The Physics of Liquid Crystals* (Clarendon, Oxford, 1993).

[3] See, for instance, P.C. Matthews, R.E. Mirollo, and S.H. Strogatz, Physica D **52**, 293 (1991).

[4] H. Cháte and P. Manneville , Phys. Rev. Lett. **58**, 112 (1987).

[5] G. Hartung, F.H. Busse, and I. Rehberg, Phys. Rev. Lett. **66**, 2741 (1991).

[6] R. Schmitz and W. Zimmermann (unpublished).

[7] A.C. Newell and J.A. Whitehead, J. Fluid Mech. **38**, 279 (1969); A.C. Newell, T. Passot, and J. Lega, Annu. Rev. Fluid Mech. **25**, 399 (1992).

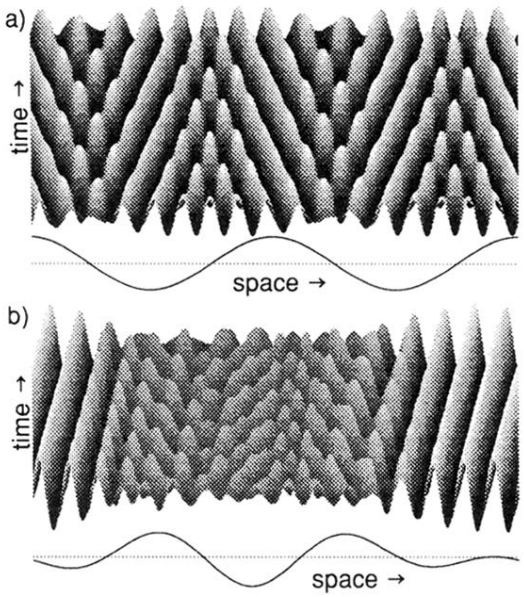


FIG. 4. The solution $u(x,t)$ of Eq. (1) is shown just above a Hopf bifurcation in a space-time plot. As shown in part (a) $u(x,t)$ is periodic in time for a single periodic modulation $M(x)$ and aperiodic for a two periodic modulation $M(x)$ as shown in part (b).